Duality of Nrf2 in iron-overload cardiomyopathy

Enrica Federti,[1] Francesca Vinchi,[2,3] Iana Iatcenko,[1] Alessandra Ghigo,[4] Alessandro Matte,[1] Serge Cedrick Mbiandjeu Toya,[1] Angela Siciliano,[1] Deborah Chiabrando,[4] Emanuela Tolosano,[4] Steven Zebulon Vance,[2] Veronica Riccardi,[1] Immacolata Andolfo,[5,6] Manuela Iezzi,[7] Alessia Lamolinara,[7] Achille Iolascon[5,6] and Lucia De Franceschi[1]

[1]Department of Medicine, University of Verona and AOUI Verona, Verona, Italy; [2]Iron Research Laboratory, Lindsley Kimball Research Institute, New York Blood Center, New York, NY, USA; [3]Department of Pathology and Laboratory Medicine, Weill Cornell Medicine, New York, NY; [4]Department Molecular Biotechnology and Health Sciences, Molecular Biotechnology Center "Guido Tarrone", University of Torino, Torino, Italy; [5]Department of Molecular Medicine and Medical Biotechnologies, Federico II University of Naples, Naples, Italy; [6]CEINGE - Biotecnologie Avanzate, Naples, Italy and [7]Department of Medicine and Aging Science, "G. d'Annunzio" University of Chieti, Chieti, Italy

Correspondence: L. De Franceschi
lucia.defranceschi@univr.it

Received: August 30, 2022.
Accepted: January 17, 2023.
Early view: January 26, 2023.

https://doi.org/10.3324/haematol.2022.281995

SUPPLEMENTAL MATERIALS

SUPPLEMENTARY METHODS

Transthoracic Echocardiography. Mice were anesthetized by isoflurane inhalation (2%), maintained by mask ventilation (isoflurane 1%) and placed in a shallow left lateral decubitus position, with strict thermoregulation (37+-1°C) to optimize physiological conditions and reduce hemodynamic variability. Echocardiographic parameters were measured at the level of the papillary muscles in the parasternal short-axis view (M mode). LV fractional shortening was calculated as follows: FS = ((LVEDD - LVESD)/ LVEDD) X 100, where LVFS indicates LV fractional shortening; LVEDD, LV end-diastolic diameter; and LVESD, LV end-systolic diameter. LV ejection fraction was calculated automatically by the echocardiography system. Diastolic parameters were measured with tissue Doppler and pulsed wave Doppler techniques in the apical long-axis view. From the pulsed wave Doppler spectral waveforms, we measured the peak early- and late-diastolic transmitral velocities (E and A waves) to obtain the E/A ratio and E-wave deceleration time. All measurements were averaged on 3 consecutive cardiac cycles per experiment and cardiac function was assessed when heart rate was 400-450 bpm. (24)

Immunohistochemistry for Ferroportin. Heart sections were rehydrated and treated for 10 min with 3% H_2O_2 (Sigma Aldrich) to block endogenous peroxidases. After washing in distilled water, tissue slides were subjected to microwave-mediated antigen retrieval using the Citraplus reagent (Biogenex). After 30 min of cooling, slides were washed three times in PBS and subjected to immune-recognition using the Vectastain ABC mouse and rabbit kits (Vector Labs) following manufacturer's instructions. Immunohistochemistry was performed using antibodies against FPN

(MTP11-A, Alpha Diagnostic Intl.). Isotype antibodies were used at the same concentration as the primary antibodies to control for antibody specificity. Slides were developed using the Vector AEC substrate (Vector labs), rinsed with distilled water, and mounted using the VectaMount AQ mounting medium (Vector Labs). Images were digitally acquired with an Echo Revolve RVL-100-G microscope (24). Ferroportin staining was quantified by measuring the intensity of brown staining on heart sections via Image J software.

Heart iron concentration (HIC). HIC was measured using the bathophenatroline sulfonate method with minor changes (24). Briefly hearts from both mouse strains were harvested, immediately ex-vivo perfused with PBS, and dried at 90°C for 20 hours. Dry hearts were smashed, weighted and digested in 1 ml of acidic solution (3M hydrochloric acid (HCl) and 10% (0.6M) trichloroacetic acid) for 20 h at 65°C. Non-heme iron was stained with the BPS chromogen reagent (5 volumes of water, 5 volumes of saturated sodium acetate and 1 volume of 0.1% bathophenanthroline sulfonate/1% thioglycolic acid). Absorbance was measured spectrophotometrically at 535 nm and concentration was calculated plotting the values onto a standard curve.

RNA isolation, cDNA synthesis, and quantitative qRT-PCR. Quantitative RT-PCR (qRT-PCR) was performed by the SYBR-green method, following standard protocols with an Applied Biosystems ABI PRISM 7900HT Sequence Detection system. Relative gene expression was calculated using the 2-DCt method, where DCt indicates the differences in the mean Ct between selected genes and the normalization control (b-actin). The qRT-PCR primers for each gene were designed

using Primer Express software version 2.0 (Life Technologies). Primers used are reported in Table 1S.

Immunoblot analysis. Frozen heart and aorta from each studied group were homogenized and lysed with iced lyses buffer (150 mM NaCl, 25 mM bicine, 0.1% SDS, 2% Triton X-100, 1 mM EDTA, protease inhibitor cocktail tablets (Roche), 1 mM Na3VO4 final concentration) then centrifuged 30 min at 4°C at 12,000 g (23-28). Specific antibodies used are: anti ANP (dilution 1:500, 75 µgr/ul loaded; Gene Tex, Irvine, CA, USA); anti Catalase from AbCam, Cambridge, UK (dilution 1:1000, 40 µgr/ul loaded); anti Nqo1 from Santa Cruz Biotechnology, Inc, CA, USA (clone C-19; dilution 1:1000, 75 µgr/ul loaded); anti SOD1 from Santa Cruz Biotechnology, Inc, CA, USA (clone C-19; dilution 1:1000, 75 µgr/ul loaded); anti Gpx1 from Santa Cruz Biotechnology, Inc, CA, USA (clone N-20; dilution 1:1000, 75 µgr/ul loaded); anti SERCA2 ATPase from Invitrogen (Thermo Fisher Scientific Inc) (dilution 1:500, 50 µgr/ul loaded); anti Phospho (Ser536) NF-kB p65 (dilution 1:1000, 75 µgr/ul loaded) and anti NF-kB p65 (clone C22B4) (dilution 1:1000, 75 µgr/ul loaded) from Cell Signaling Technology (Danvers, MA, USA); anti Endothelin-1 (ET-1) form AbCam, Cambridge, UK (dilution 1:1000, 75 µgr/ul loaded); anti ICAM-1 (clone YN1.17) was kindly gifted by dr. Gabriella Costantin (dilution 1:1000, 75 µgr/ul loaded); anti VCAM-1 from R and D Systems, Minneapolis, MN, USA (dilution 1:1000, 40 µgr/ul loaded); anti PDGF from AbCam, Cambridge, UK (dilution 1:1000, 75 µgr/ul loaded); anti Phospho (Tyr740) PDGF Receptor (PDGFR) (dilution 1:1000, 75 µgr/ul loaded), anti PDGF Receptor (PDGFR) (dilution 1:1000, 75 µgr/ul loaded); anti Phospho (Tyr653/654) FGF Receptor1 (FGFR) (dilution 1:1000, 75 µgr/ul loaded), anti FGF Receptor (FGFR) (dilution 1:1000, 75 µgr/ul loaded) from GeneTex, Inc; anti-

Ubiquitin (linkage-specific K48) form AbCam, Cambridge, UK (clone EP0589, dilution 1:1000, 75 µgr/ul loaded); anti ATF6 from Novus Biologicals Europe, Abingdon, UK (clone 70B1413.1, dilution 1:1000, 75 µgr/ul loaded); anti GADD34 form AbCam, Cambridge, UK (dilution 1:1000, 75 µgr/ul loaded); anti CHOP from Invitrogen (Thermo Fisher Scientific Inc) (clone 9C8, dilution 1:1000, 75 µgr/ul loaded); anti Nrf2-phospho-S40 (Clone EP1809Y, dilution 1:1000, 75 µgr/ul loaded, AbCam, Cambridge, UK); anti-Nrf2 (dilution 1:1000, 75 µgr/ul loaded, AbCam, Cambridge, UK); anti Heme oxygenase 1 (HO-1, clone A-3, Santa Cruz Biotechnology, Inc) (dilution 1:1000, 50 µgr/ul loaded); anti MMP 2 and anti MMP9 from GeneTex, Inc (dilution 1:1000, 75 µgr/ul loaded); anti pro Caspase 3 form AbCam, Cambridge, UK (clone E83-103; dilution 1:1000, 75 µgr/ul loaded); anti GAPDH from Santa Cruz Biotechnology, Inc, CA, USA (dilution 1:5000, 20 µgr/ul loaded). Secondary donkey anti-rabbit IgG (dilution 1:10000) and anti-mouse IgG (dilution 1:5000) HRP conjugated were from GE Healthcare Life Sciences (Little Chalfont, UK); secondary donkey anti goat IgG (dilution 1:10000) HRP conjugated was from SCBT, secondary donkey anti rat IgG (dilution 1:5000) HRP conjugated was from AbCam. Blots were developed with Luminata Forte Chemiluminescent HRP Substrate from Merk Millipore (Burlington, MA, USA), and images were acquired with the Alliance Q9 Advanced imaging system (Uvitec, UK). Densitometric analyses were performed with the Nine Alliance software (Uvitec, UK). (IP) assays were carried out using anti-TGF beta Receptor I from AbCam, Cambridge, UK. GAPDH on whole cell lysate (WCL) was used as loading control as previously reported. Oxidized proteins were monitored by using the Oxyblot Protein Oxidation Detection Kit (EMD Millipore) following the manufacturer instructions. (27, 28)

Heart Mmp9 activity and caspase 3 activity. Frozen hearts were homogenized with the Tissue Master 125 Watt Lab Homogenizer (Omni International, Bedford, USA) in tris lysis buffer (50mM tris pH7.4 and 0,5% Triton, without protease inhibitors) and proteins were used for MMP zymogram analysis, as previously described. Briefly, proteins were separated by SDS-PAGE, under non-reducing conditions, on a 7.5% T polyacrylamide gel, added of type A porcine gelatine (2 mg/ml, Merck Group, Darmstadt, Germany), polymerized within the matrix. At the end of the SDS-PAGE, gels were washed 4 times with the washing solution (50 mM Tris-HCl pH 7.4, 2.5% Triton X-100, mM CaCl2, 1 μM ZnCl2), to remove SDS, and incubated in the reacting solution (50 mM Tris-HCl pH 7.4, 1% Triton X-100, mM CaCl2, 1 μM ZnCl2) at 37 °C for 48 hrs. After the incubation, gels were stained with Colloidal Coomassie, the activity of MMPs were detected as light bands on a dark background. Images were acquired using the Alliance Q9 Advanced Chemiluminescence Imager (Uvitec, Cambridge, UK).
Heart Caspase 3 activity was determined using the CPP32/Caspase-3 Fluorometric protease assay (BioVision, Milpitas, CA, USA), following the manufacturer's instructions.

NTBI Measurement. Non-transferrin bound iron (NTBI) measurement was conducted using the ultrafiltration method. 90μl of serum were incubated with 10 μl of 800 mM nitrilotriacetic acid (NTA) containing 20μM Fe (pH 7.0) at 23°C for 30 minutes. The mixture was then ultra-filtered at 10000 g at 4ºC for 60 minutes using 10 kDa molecular weight cut-off Amicon Ultra 0.5 ml filtration units (Millipore). Clear ultrafiltrate was recovered containing NTA-mobilized iron and iron content was determined by the bathophenanthroline disulphonic acid (BDA) method. After 30

minute-incubation with a 1:1 mixture of 60mM BDA and 120mM thioglycolic acid, absorbance at 537 nm and iron concentration was quantitated by interpolation from a standard curve. Standards were prepared using iron for atomic absorption spectrometry (#16596, Sigma-Aldrich) in 80 mM NTA (0-20μM). The 800mM NTA solution used was previously treated with 20 μM iron to normalize the background iron that contaminates reagents. Thus, the zero standard contains the added background iron and gives a positive signal. When unsaturated Tf is present in sera, this additional background iron can be donated to vacant Tf sites resulting in a loss of the background signal and yielding a negative NTBI value. Values are expressed as μM NTBI.

Zymogram analysis and Caspase 3 activity. Frozen hearts were homogenized with the Tissue Master 125 Watt Lab Homogenizer (Omni International, Bedford, USA) in tris lysis buffer (50mM tris pH7.4 and 0,5% Triton, without protease inhibitors) and proteins were used for MMP zymogram analysis, as previously described. (30) Briefly, proteins were separated by SDS-PAGE, under non-reducing conditions, on a 7.5% T polyacrylamide gel, added of type A porcine gelatine (2 mg/ml, Merck Group, Darmstadt, Germany), polymerized within the matrix. At the end of the SDS-PAGE, gels were washed 4 times with the washing solution (50 mM Tris-HCl pH 7.4, 2.5% Triton X-100, mM CaCl2, 1 μM ZnCl2), to remove SDS, and incubated in the reacting solution (50 mM Tris-HCl pH 7.4, 1% Triton X-100, mM CaCl2, 1 μM ZnCl2) at 37 °C for 48 hrs. After the incubation, gels were stained with Colloidal Coomassie, the activity of MMPs were detected as light bands on a dark background. Images were acquired using the Alliance Q9 Advanced Chemiluminescence Imager (Uvitec, Cambridge, UK).

Caspase 3 activity in mouse hearts were analyzed using the CPP32/Caspase-3 Fluorometric protease assay (BioVision, Milpitas, CA, USA), following the manufacturer's instructions. Samples were read using a Victor X-4 Multilabel Plate Reader (Perkin Elmer, Waltham, United States).

Table 1S. Primers used in the present study.

Gene	Forward Primer Sequence (5'→ 3')	Reverse Primer Sequence (5'→ 3')
Il-1β	GCTGAAAGCTCTCCACCTCAA	TTGTCGTTGCTTGGTTCTCCT
Hamp	GCCTGAGCAGCACCACCTAT	TTCTTCCCCGTGCAAAGGCT
Ncx1	TAAGAAGACGAACCTGGCCC	TCATCGTCATCTTCCCCAGC
Id1	CACTGAGGGACCAGATGGACTC	GGTGGCTGCGGTAGTGTCTT
Il-6	GCCAGAGTCCTTCAGAGAGA	TGGAAATTGGGGTAGGAAGGA
Nec1	GGCTGCTGGTATCTTTGCTC	GGTCGTACTCAGAGGTCCAG
Bmp2	CGCAGCTTCCATCACGAA	CGTCACTGGGGACAGAACTT
Bmp6	GCATTTACCAAGTCTTGCAGGA	TCCAGCCAACCTTCTTCTGA
Tnnt2	GGCTCTGTCCAACATGATGC	TCTCTGTCTGTCTCTTCCCAC
GAPDH	CCACATCGCTCAGACACCAT	AGTTAAAAGCAGCCCTGGTGAC

Table 2S. Echocardiographic parameters of aged wild-type (WT) and Nrf2$^{-/-}$ mice

	WT	Nrf2$^{-/-}$
n	5	8
FS (%)	33.2± 0.9	24.6± 2.7*
EF (%)	62.0± 1.1	48.0±4.8*
IVSd (mm)	0.75± 0.05	0.69±0.03
IVSs (mm)	1.30± 0.08	1.05± 0.07
LVPWd (mm)	0.74±0.05	0.74±0.04
LVPWs (mm)	1.16± 0.09	0.98±0.06
LVIDd (mm)	4.18± 0.18	4.77±0.12*
LVIDs (mm)	2.87± 0.11	3.60±0.16**
LVW/BW (mg/g)	3.1± 0.4	3.2±0.3
LVOT CO (ml/min)	27.3± 3.3	39.6±6.6
LVOT SV (ml)	65.7± 7.4	94.2± 16.0
IVRT (ms)	17.6±1.4	17.7± 1.5
MPI	0.67±0.02	0.72± 0.07
MVDT (ms)	27.8±1.7	20.6± 1.6*
MV E/A	1.82± 0.20	2.80± 0.85

Data are shown as mean ± SEM. WT vs Nrf2$^{-/-}$: *P<0.05 and **P<0.01 by Mann Whitney test.

Abbreviations: FS, fractional shortening; EF, ejection fraction; IVSd, interventricular septal thickness at end-diastole; IVSs, interventricular septal thickness at end-systole; LVPWd, left ventricular posterior wall thickness at end-diastole; LVPWs, left ventricular posterior wall thickness at end-systole; LVEDd, left ventricular end-diastolic diameter; LVEDs, left ventricular end-systolic diameter; LVW, left ventricle weight; BW, body weight; LVOT CO, left ventricle outflow tract cardiac output; LVOT SV, left ventricle outflow tract stroke volume; IVRT, isovolumetric relaxation time; MPI, myocardial performance index; MVDT, mitral valve deceleration time; MV E/A, mitral valve E/A.

Table 3S. Echocardiographic parameters of wild-type (WT) and Nrf2$^{-/-}$ mice upon iron overload (IO).

	WT	WT IO	Nrf2$^{-/-}$	Nrf2$^{-/-}$ IO
n	4	6	8	7
FS (%)	33.7± 0.9	36.3± 1.7	24.6± 2.7*	35.9± 0.6##
EF (%)	62.6± 1.1	66.0± 2.2	48.0±4.8*	65.9± 0.8##
IVSd (mm)	0.77± 0.06	0.78± 0.03	0.69±0.03	0.84±0.03#
IVSs (mm)	1.33± 0.09	1.30± 0.03	1.05± 0.07*	1.39± 0.04##
LVPWd (mm)	0.77±0.06	0.81±0.03	0.74±0.04	0.79±0.03
LVPWs (mm)	1.20± 0.11	1.25± 0.05	0.98±0.06	1.23± 0.03#
LVIDd (mm)	4.43± 0.22	4.44± 0.08	4.77±0.12	4.26± 0.09#
LVIDs (mm)	2.94± 0.12	2.83± 0.11	3.60±0.16**	2.73±0.07###
LVW/BW (mg/g)	3.3± 0.4	3.8± 0.1	3.2±0.3	3.1±0.5
LVOT CO (ml/min)	28.0± 4.2	47.7± 8.2	39.6±6.6	36.9±4.3
LVOT SV (ml)	68.9± 8.7	113.39±14.6	94.2±16.0	93.0±7.4
MPI	0.68± 0.03	0.67± 0.03	0.72± 0.07	0.67± 0.03
MVDT (ms)	27.6± 2.1	19.5±1.7#	20.6± 1.6*	22.2±1.3
MV E/A	1.82± 0.20	1.5±0.2	2.80± 0.85	1.5± 0.1

Data are shown as Mean ± SEM. WT vs Nrf2$^{-/-}$: *P<0.05 and **P<0.01 by one-way ANOVA. IO vs untreated within each group: #P<0.05, ##P<0.01 and ###P<0.001 by one-way ANOVA.

Abbreviations: FS, fractional shortening; EF, ejection fraction; IVSd, interventricular septal thickness at end-diastole; IVSs, interventricular septal thickness at end-systole; LVPWd, left ventricular posterior wall thickness at end-diastole; LVPWs, left ventricular posterior wall thickness at end-systole; LVEDd, left ventricular end-diastolic diameter; LVEDs, left ventricular end-systolic diameter; LVW, left ventricle weight; BW, body weight; LVOT CO, left ventricle outflow tract cardiac output; LVOT SV, left ventricle outflow tract stroke volume; IVRT, isovolumetric relaxation time; MPI, myocardial performance index; MVDT, mitral valve deceleration time; MV E/A, mitral valve E/A.

SUPPLEMENTARY FIGURES

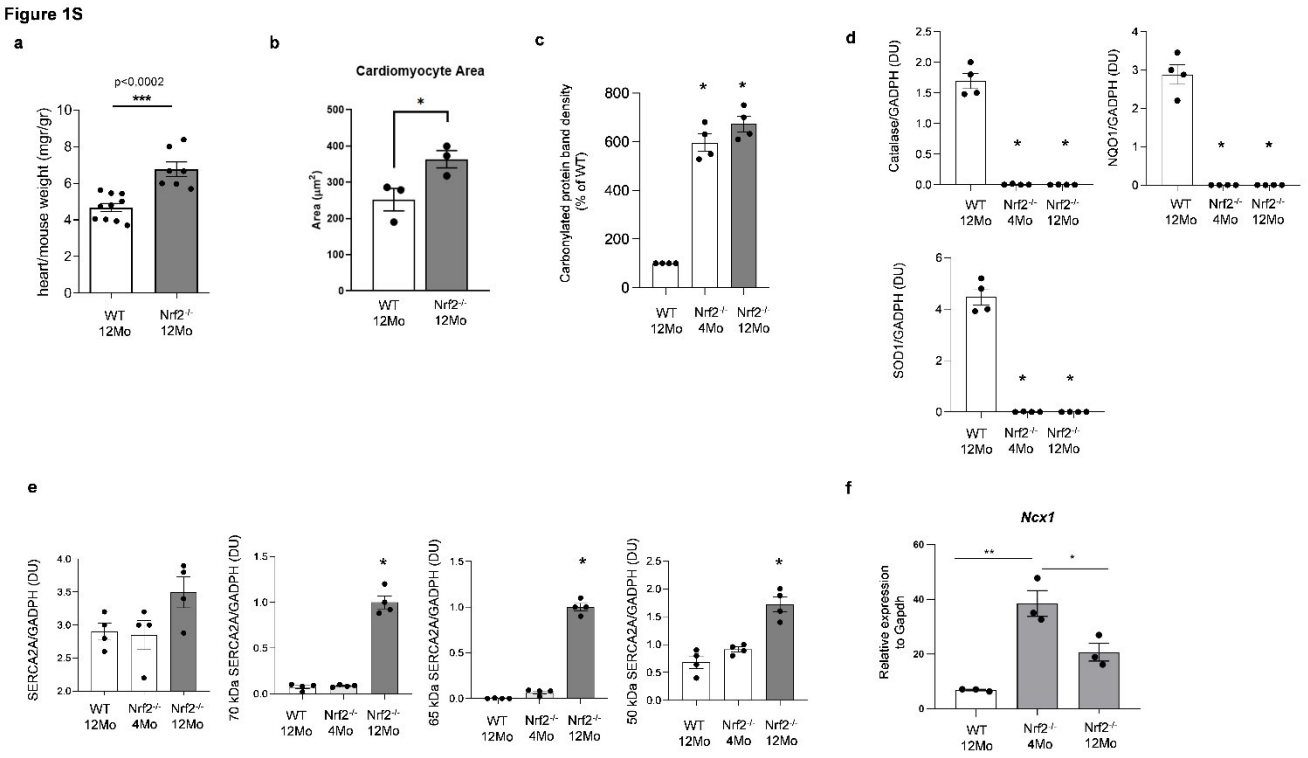

Figure 1S. (a) Heart weight to mouse weight ratio in 12 months old (12Mo) wild-type (WT) and Nrf2$^{-/-}$ mice (***p < 0.0002, compared to WT mice). **(b)** Quantification of the average cardiomyocyte area in 12 months old (12Mo) wild-type (WT) and Nrf2$^{-/-}$ mice (*p < 0.05, compared to WT mice). **(c)** Densitometric analysis Figure 1c. Data are presented as means ±SEM (*n*=4); * p<0.05 compared to wild-type (WT) mice. **(d)** Densitometric analysis Figure 1d. Data are presented as means ±SEM (*n*=4); * p<0.05 compared to wild-type (WT) mice; (DU: Densitometric Unit). **(e)** Densitometric analysis Figure 1e. Data are presented as means ±SEM (*n*=4); (* p<0.05 compared to wild-type (WT) mice; (DU: Densitometric Unit). **(f)** Quantification of Ncx1 mRNA levels normalized to Gapdh in the heart of WT mice, Nrf2$^{-/-}$ mice at 4 months (4Mo) and 12 months (12Mo) of age. Data are means ± standard deviation of three experiments (*p < 0.05, **p < 0.001, ANOVA test and post-hoc correction by Tukey's multiple comparison tests).

Figure 2S

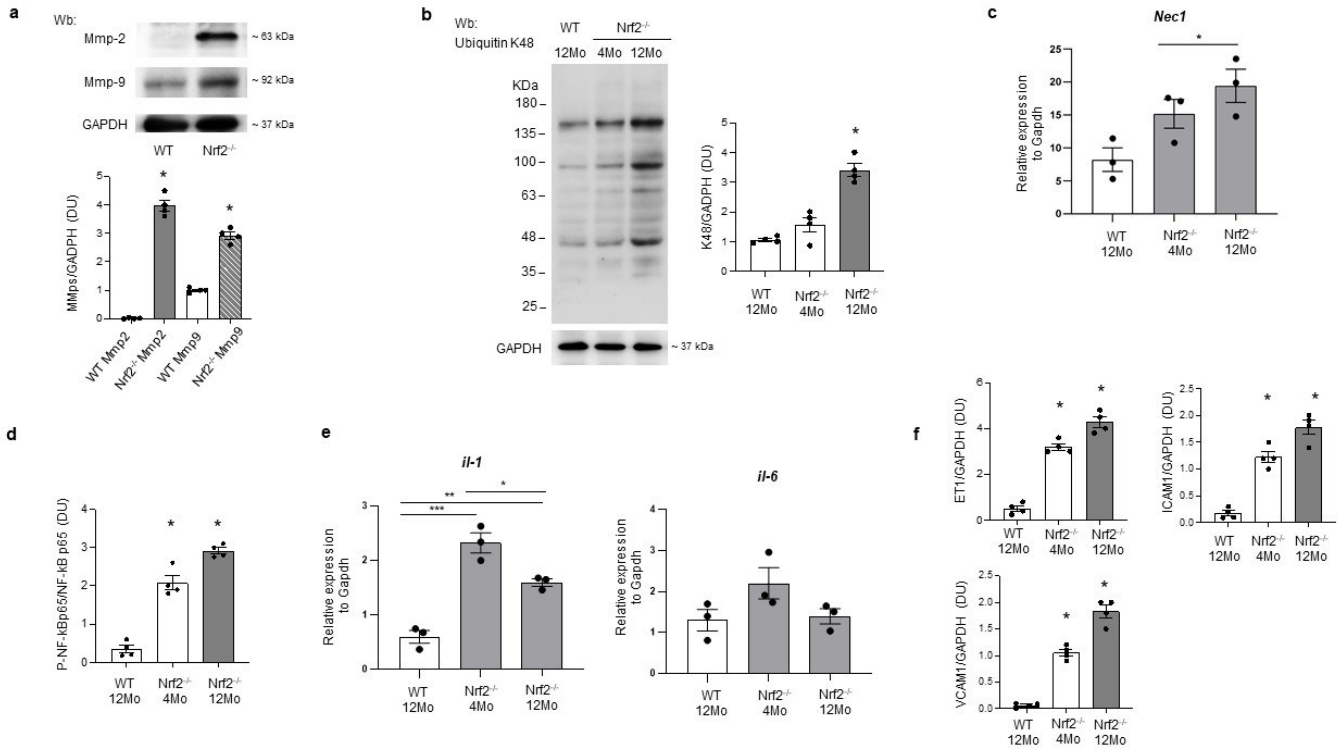

Figure 2S. (a) Immunoblot analysis using specific antibodies against Mmp-2 and Mmp-9 in heart from 12 months (12Mo) old wild-type (WT) and Nrf2$^{-/-}$ mice. GAPDH was used as protein loading control. One representative gel from 4 with similar results is shown. Densitometric analysis of immunoblot is shown on the bottom. Data are presented as means ±SEM (*n*=4); *p<0.05 compared to wild-type (WT) mice; (DU: Densitometric Unit). **(b) Left panel.** Western-blot (Wb) analysis of ubiquitinated proteins (K48) in heart from 12 months (12Mo) old wild-type (WT) mice, 4 and 12 months (Mo) old Nrf2$^{-/-}$ mice. GAPDH was used as protein loading control. **Right panel.** Quantification of band area. Data are presented as means ±SEM (*n*=4); *p<0.05 compared to wild-type (WT) mice; (DU: Densitometric Unit). **(c)** Quantification of Nec1 mRNA levels normalized to Gapdh in the heart of wild-type (WT) mice, Nrf2$^{-/-}$ mice at 4 months (4Mo) and at 12 (12Mo) months of age. Data are means ± standard deviation of three experiments (*p < 0.05, ANOVA test and post-hoc correction by Tukey's multiple comparison tests). **(d)** Densitometric analysis Figure 2a. Data are presented as means ±SEM (*n*=4); *p<0.05 compared to wild-type mice; (DU: Densitometric Unit). **(e)** Quantification of il-1 and il-6 mRNA levels normalized to Gapdh in the heart of WT mice, Nrf2$^{-/-}$ mice at 4 months (4Mo) and 12 (12Mo) months of age. Data are means ± standard deviation of three experiments (*p < 0.05, **p < 0.001, *** p < 0.00001, ANOVA test and post-hoc correction by Tukey's multiple comparison tests). **(f)** Densitometric analysis Figure 2b. Data are presented as means ±SEM (*n*=4); *p<0.05 compared to wild-type mice; (DU: Densitometric Unit).

Figure 3S

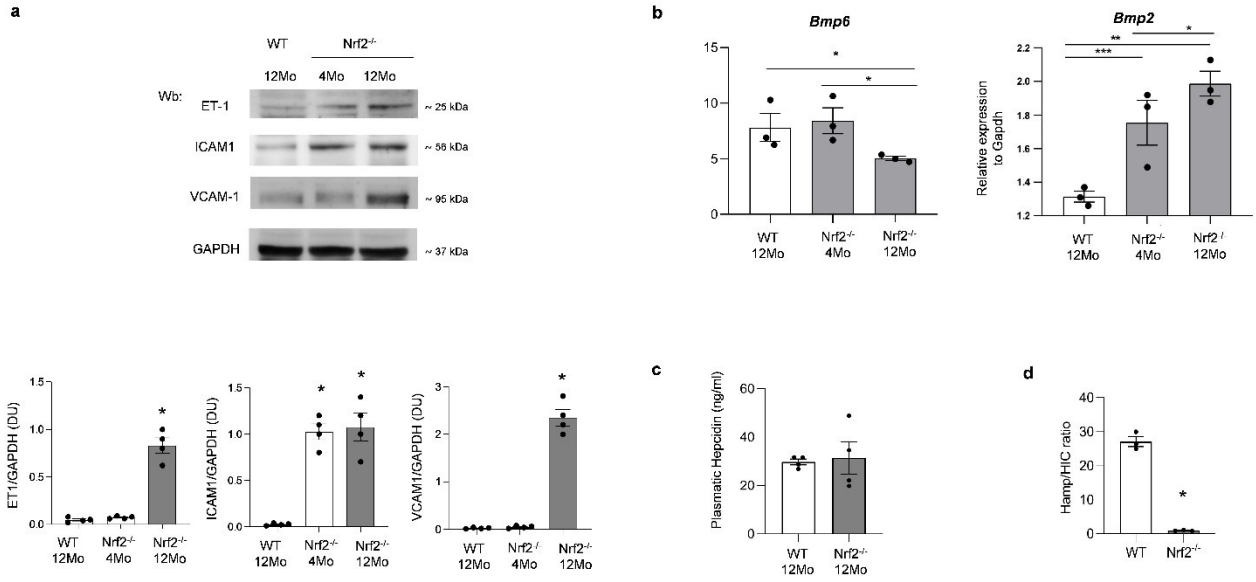

Figure 3S. (a) Immunoblot analysis using specific antibodies against ET-1, ICAM1 and VCAM1 in isolated aorta from 12 months (12Mo) old WT mice, 4 and 12 months (Mo) old Nrf2$^{-/-}$ mice. GAPDH was used as protein loading control. One representative gel from 4 with similar results is shown. Densitometric analysis of immunoblot is shown on the bottom. Data are presented as means ±SEM (*n*=4); *p<0.05 compared to wild-type mice; (DU: Densitometric Unit). **(b).** Quantification of Bmp6 and Bmp2 mRNA levels normalized to Gapdh in the heart of WT and Nrf2$^{-/-}$ mice at 4 months (4Mo) and 12 (12Mo) months of age. Data are means ± standard deviation of three experiments (*p < 0.05, **p < 0.001, *** p < 0.00001, ANOVA test and post-hoc correction by Tukey's multiple comparison tests). **(c)** Quantification of plasmatic hepcidin levels analyzed in mouse WT and Nrf2$^{-/-}$ mice at 8 months (8Mo) of age. Data are presented as means ±SEM (*n*=4); *p<0.05 compared to wild-type mice. **(d)** Hepcidin (Hamp)/ heart iron concentration (HIC) ratio in WT and Nrf2$^{-/-}$ mice at 12 (12Mo) months of age. Data are means ± SEM (n=3), *p<0.05 compared to wild-type mice.

Figure 4S

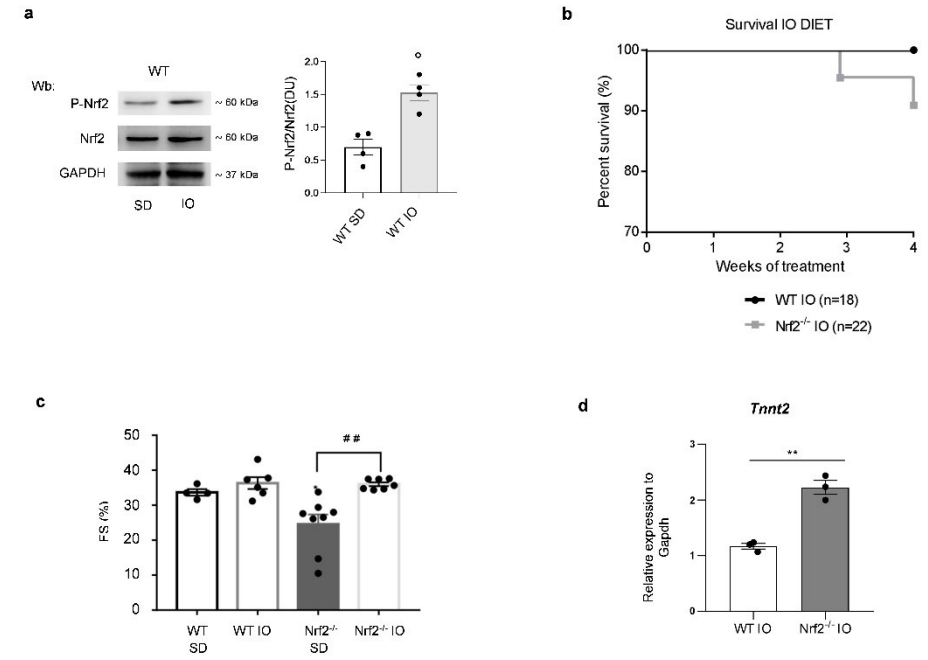

Figure 4S. (a) Immunoblot analysis using specific antibodies against p-Nrf2 and Nrf2 in heart from 12 months old WT mice exposed either to standard diet (SD) or iron overload diet (IO) for 4 weeks. GAPDH serves as protein loading control. One representative gel from 4 with similar results is shown. Densitometric analysis of immunoblot is shown on the right. Data are presented as means ±SEM (*n*=4); *p<0.05 compared to SD treated wild-type (WT) mice (DU: Densitometric Unit). **(b)** Survival of Nrf2$^{-/-}$ and wild-type (WT) mice exposed to iron overload diet (IO) for 4 weeks was assessed by long-rank test analysis (n=22 for Nrf2$^{-/-}$ IO and n=18 for WT IO). **(c)** Left ventricle fractional shortening (FS) of untreated and iron-overloaded (IO) WT and Nrf2$^{-/-}$ hearts. WT: n=4; WT IO: n=6; Nrf2$^{-/-}$: n=8; Nrf2$^{-/-}$ IO: n= 7. WT vs Nrf2$^{-/-}$: *P<0.05 and **P<0.01; IO vs untreated (standard diet) within each group: ##P<0.01 by one-way ANOVA. **(d)** Quantification of Tnnt2 mRNA levels normalized to Gapdh in the heart of WT iron overload (IO) and Nrf2$^{-/-}$ iron overload (IO) mice. Data are means ± standard deviation of three experiments (**p < 0.001, Student's t-test).

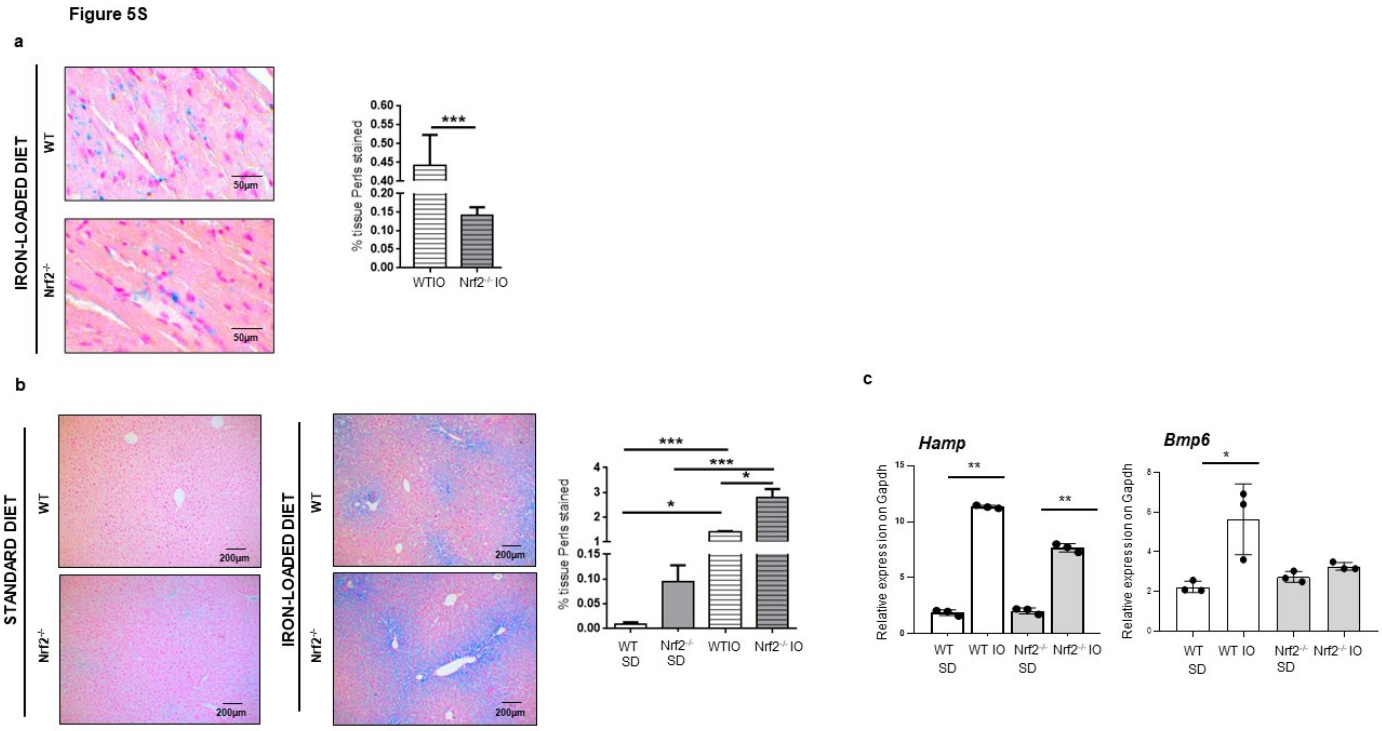

Figure 5S. (a) Perl's staining in heart tissue sections from Nrf2$^{-/-}$ and wild-type (WT) mice exposed to iron overload (IO) diet for 4 weeks. A representative picture is shown. The quantification of the % of stained tissue is shown on the right (*** $p < 0.00001$, ANOVA test and post-hoc correction by Tukey's multiple comparison tests). **(b)** Perl's staining in liver tissue sections from Nrf2$^{-/-}$ and wild-type (WT) mice exposed to a normal diet or iron overload diet (IO) for 4 weeks. A representative picture is shown. The quantification of the % of stained tissue is shown on the right (*$p < 0.05$, *** $p < 0.00001$, ANOVA test and post-hoc correction by Tukey's multiple comparison tests). **(c)** Quantification of Hamp and Bmp6 mRNA expression normalized to Gapdh in the heart of WT and Nrf2$^{-/-}$ mice on standard diet (SD) or on ironoverload diet (IO). Data are means ± standard deviation of three experiments (*$p < 0.05$, **$p < 0.001$, *** $p < 0.00001$, ANOVA test and post-hoc correction by Tukey's multiple comparison tests

Figure 6S

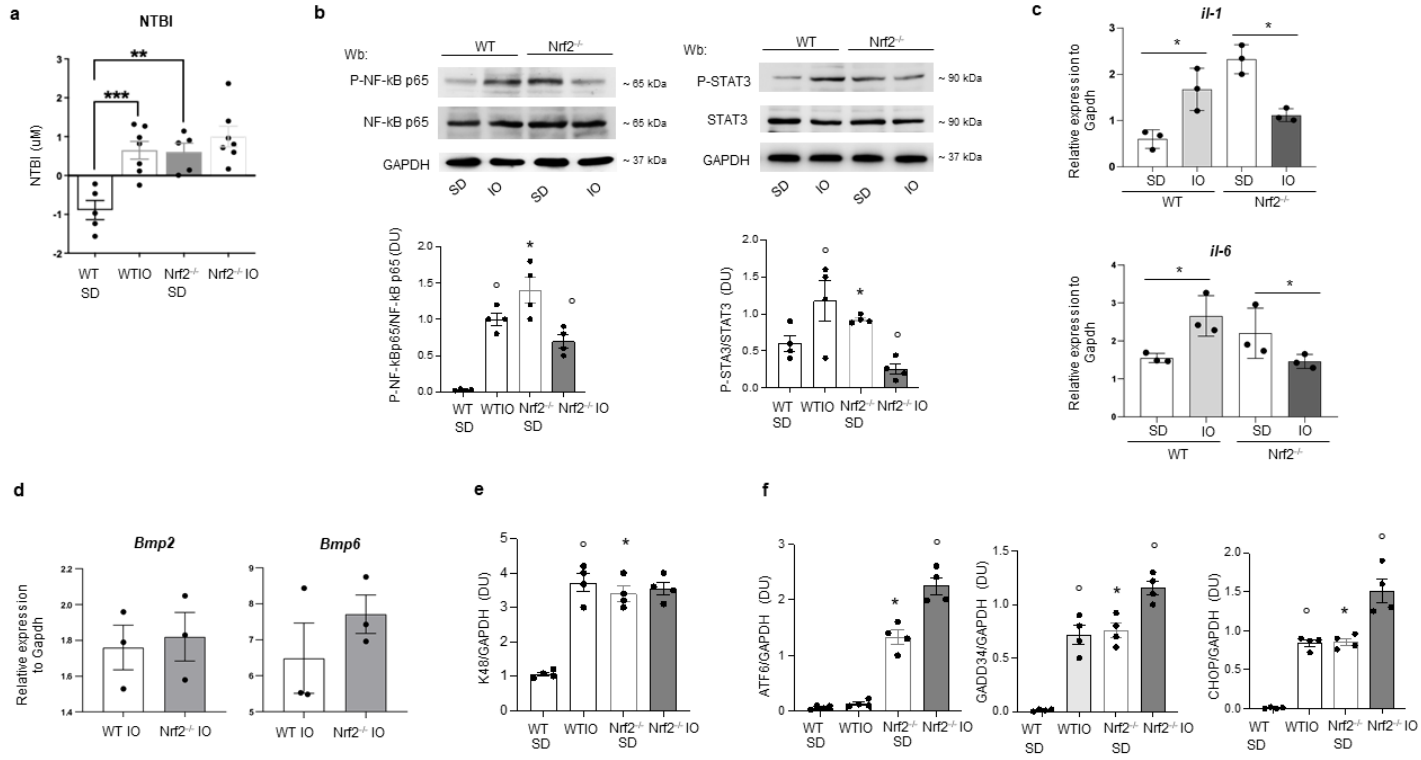

Figure 6S. (a) NTBI measurement in the serum of wild-type (WT), iron-overload (IO) WT, Nrf2$^{-/-}$, IO Nrf2$^{-/-}$ mice. (**p < 0.001, ***p < 0.00001 compared to WT mice). **(b) Left panel.** Immunoblot analysis using specific antibodies against P-NF-kB p65 in heart form 12 months old WT and Nrf2$^{-/-}$ mice exposed to standard diet (SD) or iron overload diet (IO) for 4 weeks. GAPDH was used as loading control. One representative gel from 4 with similar results is shown. Densitometric analysis of immunoblot is shown in the bottom. Data are presented as means ±SEM (*n*=4); * p<0.05 compared to SD treated WT mice; °p<0.05 compared to SD treated animals; (DU: Densitometric Unit). **Right panel.** Immunoblot analysis using specific antibodies against P-STAT3 in heart form 12 months old WT and Nrf2$^{-/-}$ mice exposed to SD or IO for 4 weeks. GAPDH serves as protein loading control. One representative gel from 4 with similar results is shown. Densitometric analysis of immunoblot is shown in the bottom. Data are presented as means ±SEM (*n*=4); * p<0.05 compared to SD treated WT mice; °p<0.05 compared to SD treated anim
als; (DU: Densitometric Unit). **(c)** Quantification of il-1 and il-6 mRNA levels normalized to Gapdh in the heart of WT, WT IO, Nrf2$^{-/-}$ and Nrf2$^{-/-}$ IO mice. Data are means ± standard deviation of three experiments (*p < 0.05, **p < 0.001, Student's t-test). **(d)** Quantification of Bmp2, and Bmp6 mRNA levels normalized to Gapdh in the heart of WT IO and Nrf2$^{-/-}$ IO mice. Data are means ± standard deviation of three experiments. **(e)** Densitometric analysis Figure 4e. Data are presented as means ±SEM (*n*=4); * p<0.05 compared to SD treated WT mice; °p<0.05 compared to SD treated animals; (DU: Densitometric Unit). **(f)** Densitometric analysis Figure 4f. Data are presented as means ±SEM (*n*=4); * p<0.05 compared to SD treated WT mice; °p<0.05 compared to SD treated animals; (DU: Densitometric Unit).

Figure 7S

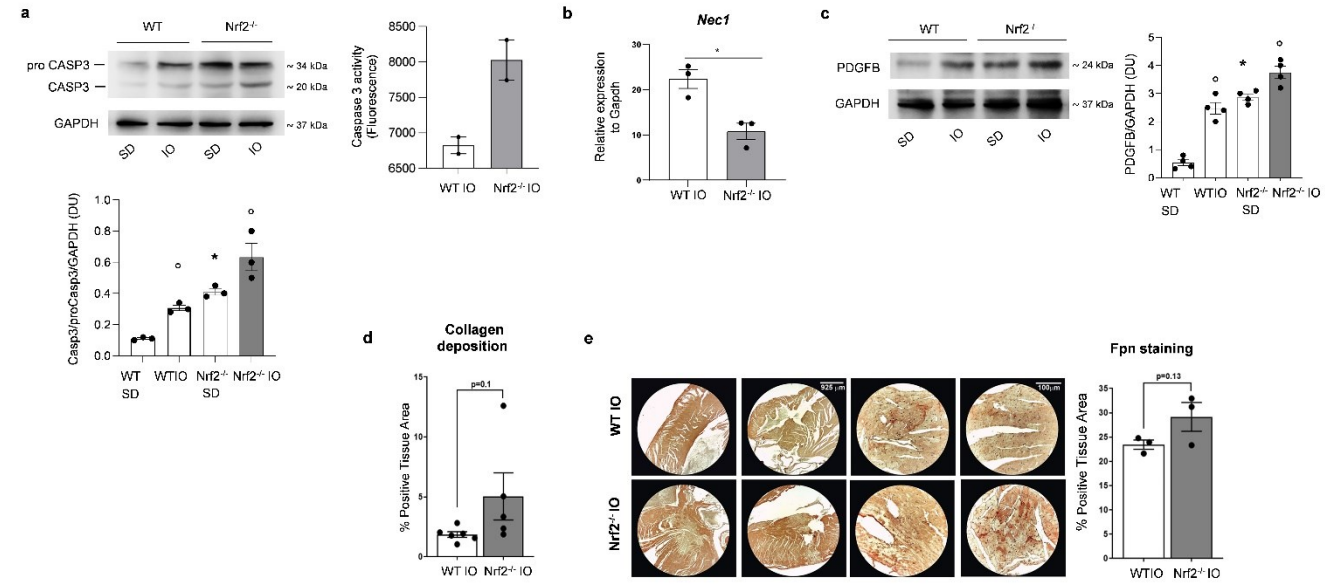

Figure 7S. (a) Left panel. Immunoblot analysis using specific antibodies against Caspase 3 in heart from 12 months old WT and Nrf2$^{-/-}$ mice exposed to standard diet (SD) or iron overload diet (IO) for 4 weeks. GAPDH serves as protein loading control. One representative gel from 3 with similar results is shown. Densitometric analysis of immunoblot is shown on the bottom. Data are presented as means ±SEM (*n*=3); * p<0.05 compared to SD treated WT mice; °p<0.05 compared to SD treated animals; (DU: Densitometric Unit). **Right panel.** Caspase 3 activity analyzed using the CPP32/Caspase-3 Fluorometric protease assay in heart from 12 months old WT and Nrf2$^{-/-}$ mice exposed to IO for 4 weeks. Data are presented as means ±SEM (*n*=2) **(b)** Quantification of Nec1 mRNA levels normalized to Gapdh in the heart of WT IO and Nrf2$^{-/-}$ IO mice. Data are means ± standard deviation of three experiments (*p < 0.05, Student's t-test). **(c)** Immunoblot analysis using specific antibodies against PDGFB in heart from 12 months old WT mice exposed to SD or IO for 4 weeks. GAPDH serves as protein loading control. One representative gel from 4 with similar results is shown. Densitometric analysis of immunoblot is shown on the right. Data are presented as means ±SEM (*n*=4); * p<0.05 compared to SD treated WT mice; °p<0.05 compared to SD treated animals; (DU: Densitometric Unit). **(d)** Quantification of collagen deposition expressed as percentage Picrosirius staining-positive tissue area on heart sections of WT and Nrf2$^{-/-}$ mice exposed to IO for 4 weeks. **(e)** Representative images of Ferroportin (Fpn) immuno-staining on heart sections of WT and Nrf2$^{-/-}$ mice exposed to IO for 4 weeks (Scale bars: 370/100µm) and relative quantification expressed as percentage positive tissue area.

Figure 8S

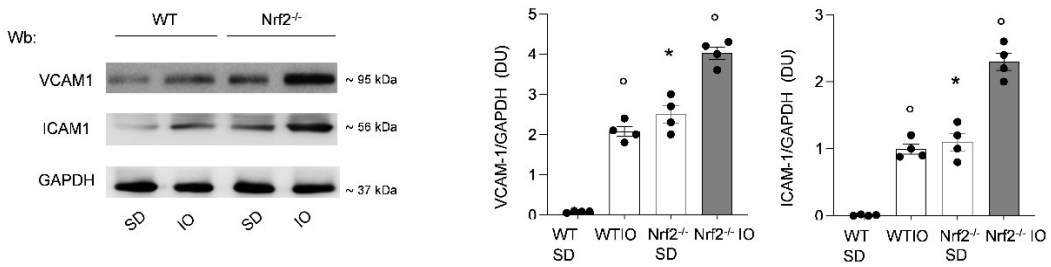

Figure 8S. Immunoblot analysis using specific antibodies against VCAM1 and ICAM1 in isolated aortas from 12 months old WT and Nrf2$^{-/-}$ mice exposed to either standard diet (SD) or iron overload diet (IO) for 4 weeks. GAPDH serves as protein loading control. One representative gel from 4 with similar results is shown. Densitometric analysis of immunoblot is shown on the right. Data are presented as means ±SEM (*n*=4); * p<0.05 compared to SD treated WT mice; °p<0.05 compared to SD treated animals; (DU: Densitometric Unit).

Figure 9S

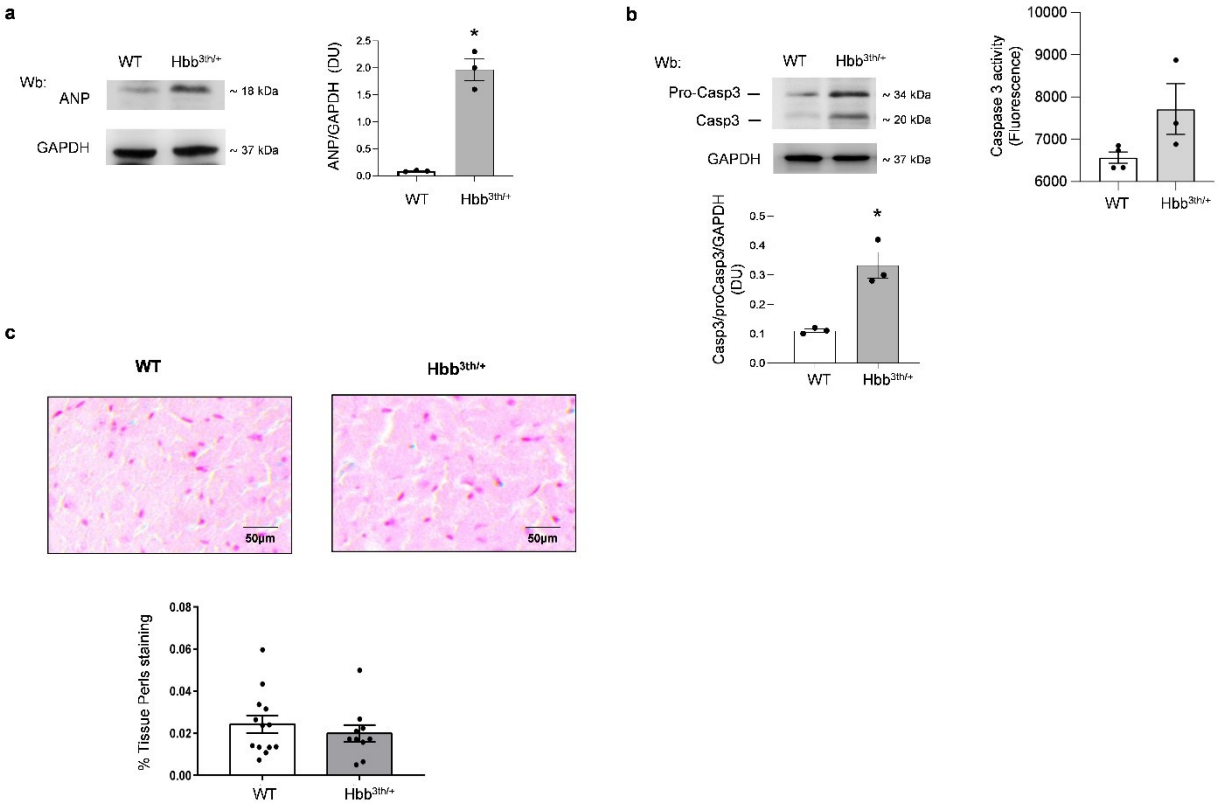

Figure 9S. (a) Immunoblot analysis using specific antibodies against ANP in heart from 12 months old WT and Hbb$^{3th/+}$ mice. GAPDH serves as protein loading control. One representative gel from 3 with similar results is shown. Densitometric analysis of immunoblot is shown on the right. Data are presented as means ±SEM (*n*=3); * p<0.05 compared to WT mice; (DU: Densitometric Unit). **(b) Left panel.** Immunoblot analysis using specific antibodies against Caspase 3 in heart from 12 months old WT and Hbb$^{3th/+}$ mice. GAPDH serves as protein loading control. One representative gel from 3 with similar results is shown. Densitometric analysis of immunoblot is shown on the right. Data are presented as means ±SEM (*n*=3); * p<0.05 compared to WT mice; (DU: Densitometric Unit). **Right panel.** Caspase 3 activity analyzed using the CPP32/Caspase-3 Fluorometric protease assay in heart from 12 months old WT and Hbb$^{3th/+}$ mice. Data are presented as means ±SEM (*n*=4-3)**. (c)** Perl's staining in heart tissue sections from 12 months old Hbb$^{3th/+}$ and wild-type (WT) animals. A representative picture is shown. The quantification of the % of stained tissue is shown on the bottom.

Figure 10S

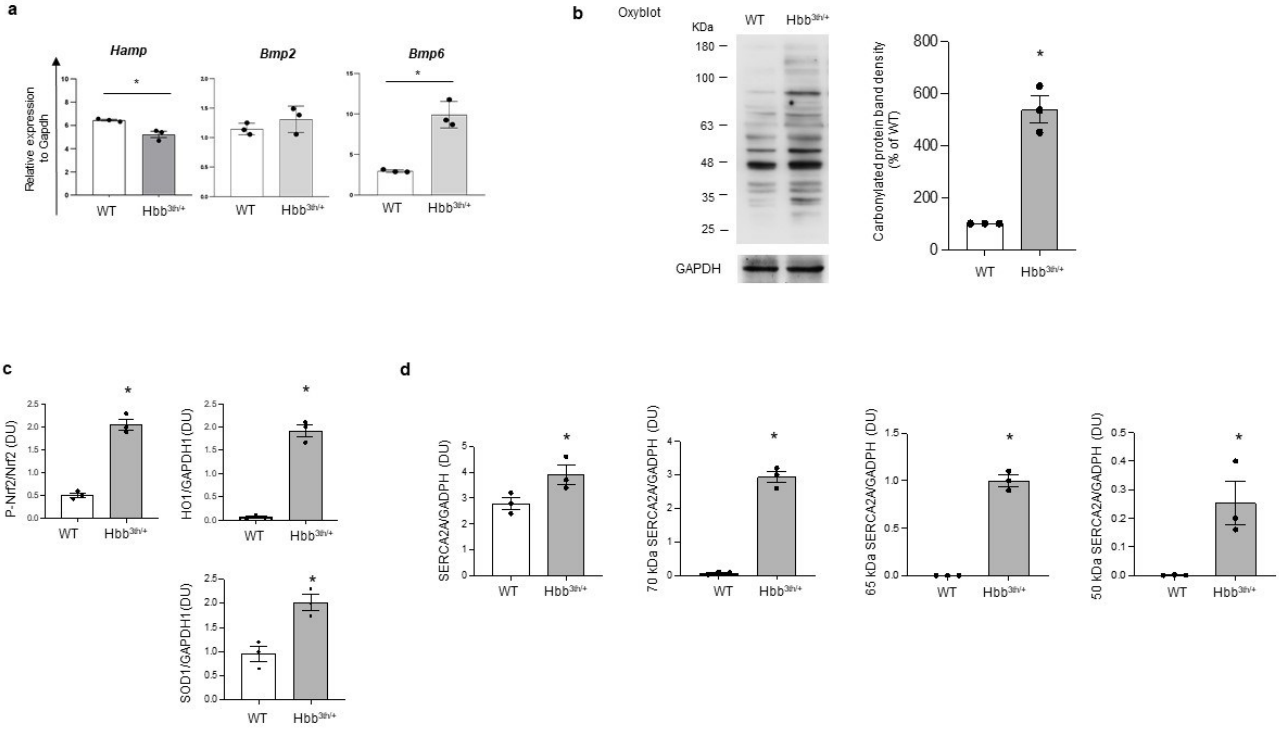

Figure 10S. (a) Quantification of Hamp, Bmp2 and Bmp6 mRNA levels normalized to Gapdh in the heart of 12 months old WT and Hbb$^{3th/+}$ mice. Data are means ± standard deviation of three experiments. (*p < 0.05, Student's t-test). **(b)** OxyBlot analysis of the soluble fractions of heart from 12 months old WT and Hbb$^{3th/+}$ mice. The carbonylated proteins (1 mg) were detected by treating with 2,4-dinitrophenylhydrazine and blotted with anti-DNP antibody. GAPDH serves as protein loading control. Densitometric analysis of immunoblots is shown on the right. Data are presented as means ±SEM (*n*=3); * p<0.05 compared to SD treated WT mice; (DU: Densitometric Unit). **(c)** Densitometric analysis Figure 5d. Data are presented as means ±SEM (*n*=3); * p<0.05 compared to SD treated WT mice; (DU: Densitometric Unit). **(d)** Densitometric analysis Figure 5e. Data are presented as means ±SEM (*n*=3); *p<0.05 compared to SD treated WT mice; (DU: Densitometric Unit).

Figure 11S

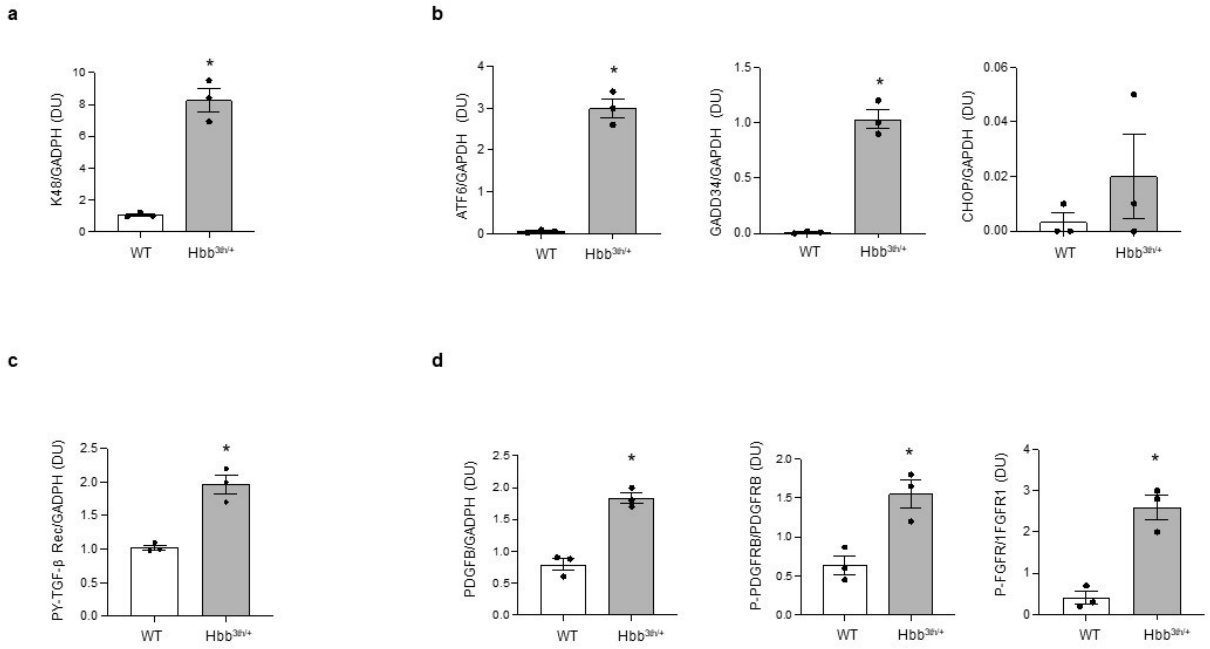

Figure 11S. (a) Densitometric analysis Figure 5f. Data are presented as means ±SEM (*n*=3); * p<0.05 compared to WT mice; (DU: Densitometric Unit). **(b)** Densitometric analysis Figure 5g. Data are presented as means ±SEM (*n*=3); * p<0.05 compared to SD treated WT mice; (DU: Densitometric Unit). **(c)** Densitometric analysis Figure 6a. Data are presented as means ±SEM (*n*=3); * p<0.05 compared to WT mice; (DU: Densitometric Unit). **(d)** Densitometric analysis Figure 6b. Data are presented as means ±SEM (*n*=3); * p<0.05 compared to WT mice; (DU: Densitometric Unit).